8-15-2019

Response of Human Small Intestinal Epithelium to Fractionated Irradiation: Dynamical Modeling Approach

Francis A. Cucinotta
University of Nevada, Las Vegas, francis.cucinotta@unlv.edu

Olga A. Smirnova
Retired

Response of Human Small Intestinal Epithelium to Fractionated Irradiation: Dynamical Modeling Approach

Authors: F. A. Cucinotta, and O. A. Smirnova

Source: Radiation Research, 192(5) : 483-492

Published By: Radiation Research Society

URL: https://doi.org/10.1667/RR15420.1

RADIATION RESEARCH **192**, 483–492 (2019)
0033-7587/19 $15.00

DOI: 10.1667/RR15420.1

Response of Human Small Intestinal Epithelium to Fractionated Irradiation: Dynamical Modeling Approach

F. A. Cucinotta[a,1] and O. A. Smirnova[b]

[a] *Department of Health Physics and Diagnostic Sciences, University of Nevada, Las Vegas, Nevada; and* [b] *Retired*

Cucinotta, F. A. and Smirnova, O. A. Response of Human Small Intestinal Epithelium to Fractionated Irradiation: Dynamical Modeling Approach. *Radiat. Res*. 192, 483–492 (2019).

A biologically motivated mathematical model of the dynamics of the small intestinal epithelium in humans treated with fractionated radiotherapy has been developed and is further investigated here. This model, originating from our previous work, is implemented as a system of nonlinear ordinary differential equations, in which the variables and parameters have a clear biological meaning. The model also includes, as input, the key parameters of fractionated irradiation. The modeling results on the dynamical response of the human normal small intestinal epithelium to fractionated radiation therapy regimens were in agreement with the corresponding empirical data, which, in turn, demonstrates the capability of the developed model for predicting the dynamics of this vital body system in humans receiving fractionated radiotherapy. It is also revealed that the cumulative damage effects of hypofractionated radiation therapy regimens on the human normal small intestinal epithelium are somewhat less pronounced than those of conventional fractionated radiation therapy regimens with the same total doses.

INTRODUCTION

The small intestinal epithelium is a critical body system in which radiation-induced damage can cause anorexia, diarrhea, dehydration and even death (*1–3*). While there are numerous quantitative studies of radiation effects on the small intestinal epithelium in laboratory animals, there is paucity of such human data (*3*). This fact makes it substantially difficult to predict, quantitatively, the response of the human small intestinal epithelium to radiation. Such predictions would be invaluable for estimating the health hazards for acutely exposed individuals in a radiation accident or incident, for astronauts exposed to unplanned radiation such as from large solar-particle events during long-term interplanetary space missions and for patients with intra-abdominal and pelvic malignancies who receive fractionated radiotherapy. In such patients, normal non-cancerous small intestinal tissue receives irradiation that can cause treatment-related side effects on this vital body system, which may in some cases lower the efficacy of radiation therapy and can significantly reduce the quality of the patient's life (*3–8*).

Thus, the study of radiation-induced damage of the human small intestinal epithelium is an actual and challenging task. To explore this issue, a mathematical model, which is capable of predicting the dynamical response of this vital body system to various radiation exposures, proves to be particularly useful, especially in view of the limited applicability of clinical methods in the investigation of radiation effects for humans.

The primary goals of the current study were to develop and investigate a biologically motivated mathematical model, which is capable of predicting the dynamics of the human small intestinal epithelium under fractionated irradiation. The model is required to account for the principal stages of the development of cells of this system and its basic kinetic and radiobiological parameters, as well as to include explicitly the key parameters of fractionated exposures (fraction doses, fraction number and time intervals between fractions). The results of this work are given below.

MATERIALS AND METHODS

Model of Dynamics of Human Small Intestinal Epithelium under Normal Conditions

In this subsection, the mathematical model of the dynamics of the small intestinal epithelium in humans under normal conditions, which is a basis for developing the model of the dynamics of this vital body system in humans exposed to irradiation, is presented. The remarkable similarity of the structure and functioning of the small intestinal epithelium in laboratory animals and humans (*1, 2*) implies that the general form of the corresponding system of nonlinear ordinary differential equations, which constitutes the model of the small intestinal epithelium for exposed humans, can be taken the same as that for unexposed mice (*1, 2*).

The model is based on conventional theories, recent concepts and facts concerning the structure and functioning of this system in

[1] Address for correspondence: University of Nevada, Las Vegas, Department of Health Physics and Diagnostic Sciences, 4505 S. Maryland Parkway, Box 453037, Las Vegas, NV 89154-3037; email: francis.cucinotta@unlv.edu.

mammals [see (*9, 10*) and references therein, as well as (*9–13*)]. Specifically, the small intestinal epithelium consists of a large number of villi and flask-shaped crypts that lie under the villous bottom. The cells of crypts and villi represent the single system of the small intestinal epithelium renewal. Basic (columnar) cells, which play an important role in nutrient absorption, prevail in this system and constitute more than 90% of the epithelial cells. Pedigree cells of the basic cells in the small intestinal epithelium are stem cells located in the crypt bottom. The stem cells are capable of self-maintaining their population, as well as of differentiating in the direction of proliferating-maturing crypt cells. The latter migrate to the top of the crypt. Close to the villous bottom, they stop to proliferate and form the pool of maturing cells. The mature cells transfer from the crypt to the villous and continue to migrate to the villous top, where they exfoliate into the intestinal lumen. It is notably that the cells of two other types (namely, goblet cells and Paneth cells, which constitute approximately 10% of the epithelial cells and are not addressed in this article) form two independent systems with their own ways of development and specific functions. In particular, goblet cells secrete mucus, which lubricates the surface of the intestinal wall, whereas Paneth cells synthesize antimicrobial peptides and proteins, thereby contributing to the protection of the body from pathogens.

The model of the dynamics of the small intestinal epithelium considers the basic (columnar) cells prevailing in the small intestinal epithelium. They are split into three compartments according to the degree of their maturity and differentiation:

1. *X*, the crypt cells capable of dividing, from the stem cell to the dividing-maturing cell;
2. *Y*, maturing crypt cells incapable of dividing;
3. *Z*, functional villous cells.

The concentrations of *X*, *Y* and *Z* cells (*x*, *y* and *z*, respectively) are used as variables of the model. Cell concentration refers to the ratio of the total number of cells of a certain group to the normal volume of the small intestinal epithelium. The corresponding system of nonlinear ordinary differential equations reads as follows (*9, 10*):

$$\frac{dx}{dt} = Bx - \gamma x, \tag{1}$$

$$\frac{dy}{dt} = \gamma x - Fy, \tag{2}$$

$$\frac{dz}{dt} = Fy - Ez. \tag{3}$$

In Eqs. (1–3), the parameters B, γ, F and E are the specific rates of the X cell reproduction, cell transfer from the group of X cells to the group of Y cells, cell transfer from the group of Y cells to the group of Z cells (i.e., cell displacement from crypt to villous) and cell leaving the group of Z cells (i.e., cell exfoliation from the villous into the intestinal lumen).

The parameter B appearing in Eq. (1) accounts for the different contributions of X, Y and Z cells to the negative-feedback control of the specific reproduction rate of X cells (*9, 10*):

$$B = \frac{\alpha}{1 + \beta\left(x + \vartheta_y y + \vartheta_z z\right)}, \tag{4}$$

where α, β, ϑ_y and ϑ_z are constants.

The parameters F and E entering Eqs. (2) and (3) depend linearly on the parameter B (*9, 10*):

$$F = \delta(1 + \sigma B), \tag{5}$$

$$E = \psi(1 + \lambda B), \tag{6}$$

with δ, σ, ψ and λ being constants.

It is found that the system (1–3) has a stable equilibrium state determined by zero values of the cell concentrations, if two parameters of the system α and γ obey the following condition: $\alpha \leq \gamma$. This stable equilibrium state can be identified with the state of complete extinction of the small intestinal epithelium. Therefore, this range of the parameters is not considered further. If $\alpha > \gamma$, then the system of equations on hand has an equilibrium state determined by the following positive values of the cell concentrations:

$$\bar{x} = \frac{(\alpha/\gamma) - 1}{\beta\left\{1 + \frac{\vartheta_y \gamma}{[\delta(1+\sigma\gamma)]} + \frac{\vartheta_z \gamma}{[\psi(1+\lambda\gamma)]}\right\}}, \tag{7}$$

$$\bar{y} = \frac{\bar{x}\gamma}{\delta(1 + \sigma\gamma)}, \tag{8}$$

$$\bar{z} = \frac{\bar{x}\gamma}{\psi(1 + \lambda\gamma)}. \tag{9}$$

The stable equilibrium state [Eqs. (7–9)] of the system of equations on hand can be identified with the homeostasis state of the small intestinal epithelium, whereas the values $\bar{z}$, $\bar{y}$ and $\bar{x}$ can be considered as the normal concentrations of villous basic (columnar) cells and their incapable and capable of dividing precursors in crypts [see (*10*) for details].

The initial conditions for Eqs. (1–3) are equal to the normal concentrations of the cells under consideration: $x(0) = \bar{x}$, $y(0) = \bar{y}$ and $z(0) = \bar{z}$, the values $\bar{x}$, $\bar{y}$, and $\bar{z}$ being determined by Eqs. (7–9).

Model of Dynamics of Small Intestinal Epithelium in Humans Exposed to Acute Irradiation

In this subsection, the mathematical model [Eqs. (1–3)] is extended to describe the dynamics of the small intestinal epithelium in acutely irradiated humans (the latter can, of course, be considered as a partial case of *n*-fractionated irradiation with $n = 1$). In this way, we apply the dynamical approach, which was elaborated and successfully employed earlier to the modeling of the effects of acute radiation on the dynamics of the young swine skin epidermal epithelium, which bears many characteristics similar to the human skin epidermal epithelium (*10, 14, 15*).

Specifically, the model of the dynamics of the small intestinal epithelium in acutely irradiated humans is based on the following radiobiological concepts and facts:

1. The one-target-one-hit theory of cell damage (*16*), according to which the damage rate of radiosensitive cells is assumed to be proportional to the dose rate N;
2. The experimental findings and the concept proposed by Bond, *et al.* (*1*) concerning the types of reaction of radiosensitive cells in renewing systems to radiation impact. According to them, the radiosensitive cells may stay undamaged, or become heavily damaged, moderately damaged and weakly damaged. Heavily damaged cells die within several hours postirradiation (interphase death). Moderately damaged cells can divide a few (at least, one) times and die within 1–2 days postirradiation (mitotic death). The weakly damaged cells are able to proliferate and differentiate as undamaged ones over a certain period of time ($0 < t \leq T_{ar}$), forming the pools of weakly damaged progenies. After the time T_{ar}, all weakly damaged cells and their progenies die within several days;
3. Experimental facts according to which the crypt cells capable of dividing (X cells) are radiosensitive to some extent, whereas the maturing crypt cells incapable of dividing (Y cells) and villous cells (Z cells) are radioresistant (*1*).

Proceeding from these concepts and facts, the radiosensitive X cells are divided into four groups:

X^{ud}, undamaged cells;
X^{hd}, heavily damaged cells that die within several hours postirradiation (interphase death);
X^{md}, moderately damaged cells that die within a few days postirradiation (mitotic death);
X^{wd}, weakly damaged cells, which function as X^{ud} cells, if the time t elapsed after irradiation does not exceed T_{ar}, i.e., $t \leq T_{ar}$, and which only die within several days, if the time t passed after irradiation exceeds T_{ar}, i.e., $t > T_{ar}$.

In turn, Y cells are divided into two groups:

Y^{ud}, progenies of X^{ud} cells;
Y^{wd}, progenies of X^{wd} cells, which function as Y^{ud} cells, if $t \leq T_{ar}$, and which only die within several days, if $t > T_{ar}$.

Finally, Z cells are divided into two groups:

Z^{ud}, progenies of Y^{ud} cells;
Z^{wd}, progenies of Y^{wd} cells, which function as Z^{ud} cells, if $t \leq T_{ar}$, and which only die within several days, if $t > T_{ar}$.

In constructing the model, we assume the following: 1. The dynamics of X^{ud} cells and the dynamics of X^{wd} cells (if $t \leq T_{ar}$) are determined by the rates of their reproduction and transition to the groups of Y^{ud} and Y^{wd} cells, respectively; 2. The dynamics of Y^{ud} and the dynamics of Y^{wd} cells (if $t \leq T_{ar}$) are determined by the rate of their arrival from the groups of X^{ud} and X^{wd} cells and by the rate of their transfer to the groups of Z^{ud} and Z^{wd} cells, respectively; 3. The dynamics of Z^{ud} cells and the dynamics Z^{wd} cells (if $t \leq T_{ar}$) are determined by the rate of their arrival from the groups of Y^{ud} cells and Y^{wd} cells and by the rate of leaving the groups of Z^{ud} and Z^{wd} cells, respectively; 4. The dynamics of X^{wd}, Y^{wd} and Z^{wd} cells (if $t > T_{ar}$) is determined only by their death rate; and 5. The dynamics X^{hd} and X^{md} cells is determined only by their death rates.

The model variables are the concentrations of X^{ud}, Y^{ud}, Z^{ud}, X^{wd}, Y^{wd}, Z^{wd}, X^{md} and X^{hd}, namely, x^{ud}, y^{ud}, z^{ud}, x^{wd}, y^{wd}, z^{wd}, x^{md} and x^{hd}, respectively.

The model based on the aforementioned considerations has the following form [see also (*10, 14, 15*)]:

$$\frac{dx^{ud}}{dt} = Bx^{ud} - \gamma x^{ud}, \tag{10}$$

$$\frac{dy^{ud}}{dt} = \gamma x^{ud} - Fy^{ud}, \tag{11}$$

$$\frac{dz^{ud}}{dt} = Fy^{ud} - Ez^{ud}, \tag{12}$$

$$\frac{dx^{hd}}{dt} = -\nu x^{hd}, \tag{13}$$

$$\frac{dx^{md}}{dt} = -\mu x^{md}, \tag{14}$$

$$\frac{dx^{wd}}{dt} = \theta(T_{ar} - t)\left[Bx^{wd} - \gamma x^{wd}\right] - \theta(t - T_{ar})\eta x^{wd}, \tag{15}$$

$$\frac{dy^{wd}}{dt} = \theta(T_{ar} - t)\left[\gamma x^{wd} - Fy^{wd}\right] - \theta(t - T_{ar})\eta y^{wd}, \tag{16}$$

$$\frac{dz^{wd}}{dt} = \theta(T_{ar} - t)\left[Fy^{wd} - Ez^{wd}\right] - \theta(t - T_{ar})\eta z^{wd}. \tag{17}$$

Here the parameters B, γ, F and E are the specific rates of reproduction of X^{ud} cells and of X^{wd} cells (if $t \leq T_{ar}$) cell transition from the group of X^{ud} cells to the group of Y^{ud} cells and from the group of X^{wd} cells to the group of Y^{wd} cells (if $t \leq T_{ar}$), cell transition from the group of Y^{ud} cells to the group of Z^{ud} cells and from the group of Y^{wd} cells to the group of Z^{wd} cells (if $t \leq T_{ar}$), and cell leaving the group of Z^{ud} cells and the group of Z^{wd} cells (if $t \leq T_{ar}$). The coefficients μ and ν are the specific death rates of X^{md} and X^{hd} cells, whereas η is the specific death rate of X^{wd}, Y^{wd} and Z^{wd} cells (if $t > T_{ar}$). The coefficients γ, μ, ν and η are constants.

The function $\theta(t)$, which appears in Eqs. (15–17), is the unit step-function (*17*):

$$\theta(t) = \begin{cases} 1, t \geq 0, \\ 0, t < 0. \end{cases} \tag{18}$$

The parameter T_{ar} entering the same equations is taken as the linear function of the radiation dose D as that found elsewhere (*10, 14, 15*):

$$T_{ar} = \tau_{ar} - \upsilon D, \tag{19}$$

with the parameters τ_{ar} and υ being constants.

The parameter B appearing in Eqs. (10) and (15) is determined using the formula, which, likewise Eq. (4), accounts for the different contributions of the cells on hand to the negative-feedback control of the specific reproduction rate of X^{ud} cells and of X^{wd} cells (if $t \leq T_{ar}$) [see also (*10, 14, 15*)]:

$$B = \frac{\alpha}{1 + \beta\left[x^{ud} + \Phi_x + \phi x^{md} + \varphi x^{hd} + \vartheta_y\left(y^{ud} + \Phi_y\right) + \vartheta_z\left(z^{ud} + \Phi_z\right)\right]}, \tag{20}$$

Where

$$\Phi_x = [\theta(T_{ar} - t) + \varsigma\theta(t - T_{ar})]x^{wd}, \tag{21}$$

$$\Phi_y = [\theta(T_{ar} - t) + \varsigma\theta(t - T_{ar})]y^{wd}, \tag{22}$$

$$\Phi_z = [\theta(T_{ar} - t) + \varsigma\theta(t - T_{ar})]z^{wd}, \tag{23}$$

The function $\theta(t)$ in Eqs. (21–23) is the unit step-function [Eq. (18)]. The parameters α, β, ϑ_y, ϑ_z, ϕ, φ and ς are constants.

The parameters F and E entering Eqs. (11), (12), (16) and (17) are described using Eqs. (5) and (6), the parameter B in them being determined by Eq. (20).

The initial conditions for Eqs. (10–17) are the following [see also (*10, 14, 15*)]:

$$x^{ud}(0) = \bar{x}\exp\left(-\frac{D}{D_x^0}\right), \tag{24}$$

$$y^{ud}(0) = \bar{y}, \tag{25}$$

$$z^{ud}(0) = \bar{z}, \tag{26}$$

$$x^{hd}(0) = \bar{x}\frac{\rho}{1+\rho}\left[1 - \exp\left(-\frac{D}{D_x^0}\right)\right], \tag{27}$$

$$x^{md}(0) = \bar{x}\frac{1}{1+\rho}\frac{1}{1+\kappa}\left[1 - \exp\left(-\frac{D}{D_x^0}\right)\right], \tag{28}$$

$$x^{wd}(0) = \bar{x}\frac{1}{1+\rho}\frac{\kappa}{1+\kappa}\left[1 - \exp\left(-\frac{D}{D_x^0}\right)\right], \tag{29}$$

$$y^{wd}(0) = 0, \tag{30}$$

$$z^{wd}(0) = 0. \tag{31}$$

In these equations, $\bar{x}$, $\bar{y}$, and $\bar{z}$ are the normal concentrations of X, Y and Z cells, ρ is the ratio of the fractions of X cells, which transfer to heavily damaged X^{hd} cells and to moderately damaged X^{md} and weakly damaged X^{wd} cells, and κ is the ratio of the fractions of X cells, which transfer to weakly damaged X^{wd} cells and to moderately damaged X^{md} cells. The parameters ρ and κ are determined by the formulas as those used elsewhere (*10, 14, 15*):

$$\rho = \frac{1 - \exp(-D/D_x^{00})}{\exp(-D/D_x^{00}) - \exp(-D/D_x^{0})}, \tag{32}$$

$$\kappa = \frac{\exp(-D/D_x^{000}) - \exp(-D/D_x^{0})}{\exp(-D/D_x^{00}) - \exp(-D/D_x^{000})}. \tag{33}$$

Here, D is a dose of acute irradiation, D_x^0, D_x^{00}, and D_x^{000} are the parameters characterizing the radiosensitivity of X cells. Specifically, D_x^0 is equivalent to the conventional radiobiological dose D_0. After irradiation at such dose, the number of X cells left undamaged is $e = 2.718\ldots$ times smaller than their initial number (*1*). The coefficient D_x^{00} is the dose, after exposure to which the number of X cells that did not undergo the interphase death is $e = 2.718\ldots$ times smaller than their initial number. In turn, the coefficient D_x^{000} is the dose, after exposure to which the number of X cells that did not undergo either the interphase death or the mitotic death is $e = 2.718\ldots$ times smaller than their initial number.

Model of Dynamics of Small Intestinal Epithelium in Humans Exposed to Fractionated Irradiation

In this subsection the model [Eqs. (10–17)], which describes the dynamics of the small intestinal epithelium in humans exposed to acute radiation, is extended to describe the effects of n-fractionated irradiation on this vital body system. In this way, we use the approach, which was elaborated on and successfully applied to the modeling of the effects of n-fractionated irradiation on the young swine skin epidermal epithelium (*10, 15*). Specifically, n-fractionated irradiation is considered as a set of n acute exposures with doses D_i ($i = 1, \ldots, n$) and with time intervals between the exposures τ_i ($i = 1,\ldots, n-1$). Before the first irradiation performed at time moment $T_1 = 0$, the human small intestinal epithelium consists of undamaged X^{ud}, Y^{ud} and Z^{ud} cells, with concentrations equal to their normal values $\bar{x}$, $\bar{y}$ and $\bar{z}$, respectively. In the result of the first irradiation, a portion of undamaged X^{ud} cells remains undamaged (X^{ud} cells), whereas the other portion of the cells transfers to the groups of heavily damaged cells (X^{hd} cells), moderately damaged cells (X^{md} cells) and weakly damaged cells (X_1^{wd} cells). In turn, progenies of X_1^{wd} cells form the groups of Y_1^{wd} and Z_1^{wd} cells. Behavior of X_1^{wd}, Y_1^{wd} and Z_1^{wd} cells is the same as that for X^{ud}, Y^{ud} and Z^{ud} cells until time moment $T_1^{'} = T_{ar} + T_1 = T_{ar}$, after which the dynamics of X_1^{wd}, Y_1^{wd} and Z_1^{wd} cells is determined only by the death rate. Thus, the first irradiation leads to the appearance of five new groups of cells.

Before the second exposure performed at time moment $T_2 = \tau_1$, the human small intestinal epithelium consists of undamaged X^{ud}, Y^{ud} and Z^{ud} cells, moderately damaged X^{md} cells, heavily damaged X^{hd} cells, and weakly damaged of X_1^{wd}, Y_1^{wd} and Z_1^{wd} cells. In the result of the second irradiation, a part of undamaged X^{ud} cells remains undamaged ones (X^{ud} cells), whereas the other part of cells transfers to the groups of heavily damaged cells (X^{hd} cells), moderately damaged cells (X^{md} cells) and weakly damaged cells (X_2^{wd} cells). In turn, progenies of weakly damaged X_2^{wd} cells form the groups of weakly damaged Y_2^{wd} and Z_2^{wd} cells. Behavior of X_2^{wd}, Y_2^{wd} and Z_2^{wd} cells is the same as that of undamaged X^{ud}, Y^{ud} and Z^{ud} cells until time moment $T_2^{'} = T_{ar} + T_2 = T_{ar} + \tau_1$, after which the dynamics of X_2^{wd}, Y_2^{wd} and Z_2^{wd} cells is determined only by the death rate. In the result of the second irradiation, a portion of the weakly damaged X_1^{wd} cells is not damaged and remains as weakly damaged X_1^{wd} cells, whereas the other portion of cells is damaged additionally by radiation and, as it is supposed, transfers to the group of heavily damaged cells (X^{hd} cells). In addition, in the result of the second irradiation, a part of the moderately damaged X^{md} cells is not damaged additionally and remains moderately damaged X^{md} cells, whereas the other part of cells is damaged additionally by radiation and, as it is supposed, transfers to the group of heavily damaged cells (X^{hd} cells). Thus, the second irradiation leads to the appearance of three new groups of cells.

Before the i-th exposure performed at time moment $T_i = \tau_1 + \ldots + \tau_{i-1} = \sum_{j=1}^{i-1} \tau_j$, the human small intestinal epithelium consists of undamaged X^{ud}, Y^{ud} and Z^{ud} cells, moderately damaged X^{md} cells, heavily damaged X^{hd} cells, as well as $[3 \times (i-1)]$ groups of weakly damaged cells, namely, X_1^{wd}, Y_1^{wd}, Z_1^{wd}, X_2^{wd}, Y_2^{wd}, Z_2^{wd},..., X_{i-1}^{wd}, Y_{i-1}^{wd}, Z_{i-1}^{wd} cells. In the result of the i-th irradiation, a portion of undamaged X^{ud} cells remains undamaged (X^{ud} cells), whereas the other portion of cells transfers to the groups of heavily damaged cells (X^{hd} cells), moderately damaged cells (X^{md} cells) and weakly damaged cells (X_i^{wd} cells). In turn, progenies of X_i^{wd} cells form the groups of weakly damaged Y_i^{wd} cells and weakly damaged Z_i^{wd} cells. Behavior of X_i^{wd}, Y_i^{wd} and Z_i^{wd} cells is the same as that for undamaged X^{ud}, Y^{ud} and Z^{ud} cells until time moment $T_i^{'} = T_{ar} + T_i = T_{ar} + \sum_{j=1}^{i-1} \tau_j$, after which the dynamics of X_i^{wd}, Y_i^{wd} and Z_i^{wd} cells are determined only by the death rate. As for the groups of weakly damaged cells (X_1^{wd},..., X_{i-1}^{wd} cells), a portion of the cells of each such group remains weakly damaged ones (X_1^{wd}, ..., X_{i-1}^{wd} cells) after the i-th irradiation, whereas the other portion of cells of each such group transfers to the group of heavily damaged cells (X^{hd} cells). In addition, in the result of the i-th irradiation, a portion of the moderately damaged X^{md} cells is not further damaged and remains as moderately damaged X^{md} cells, whereas the other portion of cells is damaged additionally by radiation and transfers to the group of heavily damaged cells (X^{hd} cells). Thus, the i-th irradiation leads to the appearance of three new groups of cells; also, after n irradiations, the number of groups of cells under consideration and subsequently, the number of variables of this version of the model of the human small intestinal epithelium is equal to: $3 + 2 + 3 \times n = 5 + 3 \times n$. The concentrations of the aforementioned cells, namely, x^{ud}, y^{ud}, z^{ud}, x^{wd}, x^{md} and x^{hd}, as well as x_i^{wd}, y_i^{wd}, z_i^{wd} ($i = 1,\ldots, n$) are the model variables.

Proceeding from the foregoing assumptions, the model, which describes the dynamics of the human small intestinal epithelium under n-fractionated irradiation with doses D_i ($i = 1,\ldots, n$) and with the time intervals between irradiations τ_i ($i = 1,\ldots, n-1$), takes the following form [see also (*10, 15*)]:

$$\frac{dx^{ud}}{dt} = Bx^{ud} - \gamma x^{ud}, \tag{34}$$

$$\frac{dy^{ud}}{dt} = \gamma x^{ud} - Fy^{ud}, \tag{35}$$

$$\frac{dz^{ud}}{dt} = Fy^{ud} - Ez^{ud}, \tag{36}$$

$$\frac{dx^{hd}}{dt} = -\nu x^{hd}, \tag{37}$$

$$\frac{dx^{md}}{dt} = -\mu x^{md}, \tag{38}$$

$$\frac{dx_i^{wd}}{dt} = \theta\left(T_{ar} - t + \sum_{j=1}^{i-1} \tau_j\right)\left[Bx_i^{wd} - \gamma x_i^{wd}\right] - \theta\left(t - T_{ar} - \sum_{j=1}^{i-1} \tau_j\right)\eta x_i^{wd} \qquad (i = 1, \ldots, n), \tag{39}$$

$$\frac{dy_i^{wd}}{dt} = \theta\Big(T_{ar} - t + \sum_{j=1}^{i-1}\tau_j\Big)\big[\gamma x_i^{wd} - F y_i^{wd}\big] - \theta\Big(t - T_{ar} - \sum_{j=1}^{i-1}\tau_j\Big)\eta y_i^{wd} \qquad (i = 1, \ldots, n), \tag{40}$$

$$\frac{dz_i^{wd}}{dt} = \theta\Big(T_{ar} - t + \sum_{j=1}^{i-1}\tau_j\Big)\big[F y_i^{wd} - E z_i^{wd}\big] - \theta\Big(t - T_{ar} - \sum_{j=1}^{i-1}\tau_j\Big)\eta z_i^{wd} \qquad (i = 1, \ldots, n), \tag{41}$$

where $\theta(t)$ is the unit step-function [Eq. (18)].

In the case of n-fractionated irradiation, the specific reproduction rate B in Eqs. (34) and (39) is described in the following way [see also (*10, 15*)]:

$$B = \frac{\alpha}{1 + \beta\Big[x^{ud} + \Phi_x' + \phi x^{md} + \varphi x^{hd} + \vartheta_y\Big(y^{ud} + \Phi_y'\Big) + \vartheta_z\big(z^{ud} + \Phi_z'\big)\Big]}, \tag{42}$$

where

$$\Phi_x' = \sum_{i=1}^{n}\Big\{\Big[\theta\Big(T_{ar} - t + \sum_{j=1}^{i-1}\tau_j\Big) + \varsigma\theta\Big(t - T_{ar} - \sum_{j=1}^{i-1}\tau_j\Big)\Big] \times x_i^{wd}\Big\}, \tag{43}$$

$$\Phi_y' = \sum_{i=1}^{n}\Big\{\Big[\theta\Big(T_{ar} - t + \sum_{j=1}^{i-1}\tau_j\Big) + \varsigma\theta\Big(t - T_{ar} - \sum_{j=1}^{i-1}\tau_j\Big)\Big] \times y_i^{wd}\Big\}, \tag{44}$$

$$\Phi_z' = \sum_{i=1}^{n}\Big\{\Big[\theta\Big(T_{ar} - t + \sum_{j=1}^{i-1}\tau_j\Big) + \varsigma\theta\Big(t - T_{ar} - \sum_{j=1}^{i-1}\tau_j\Big)\Big] \times z_i^{wd}\Big\}. \tag{45}$$

Equations (42–45) account for the different contributions of all the cells under consideration to the negative-feedback control of the specific reproduction rate of X^{ud} cells and of X_i^{wd} ($i = 1, \ldots, n$) cells (at $t \le T_{ar} + \sum_{j=1}^{i-1}\tau_j$). The parameters in Eqs. (42–45) are specified above.

In the case of n-fractionated irradiation, the specific rates F and E entering Eqs. (35), (36), (40) and (41) are described by Eqs. (5) and (6), the parameter B in them being determined by Eq. (42).

The initial conditions for Eqs. (34–41) are the following [see also (*10, 15*)]:

$$x^{ud}(0) = \bar{x}\exp\Big(-\frac{D_1}{D_x^0}\Big), \tag{46}$$

$$y^{ud}(0) = \bar{y}, \tag{47}$$

$$z^{ud}(0) = \bar{z}, \tag{48}$$

$$x^{hd}(0) = \bar{x}\frac{\rho_1}{1+\rho_1}\Big[1 - \exp\Big(-\frac{D_1}{D_x^0}\Big)\Big], \tag{49}$$

$$x^{md}(0) = \bar{x}\frac{1}{1+\rho_1}\frac{1}{1+\kappa_1}\Big[1 - \exp\Big(-\frac{D_1}{D_x^0}\Big)\Big], \tag{50}$$

$$x_1^{wd}(0) = \bar{x}\frac{1}{1+\rho_1}\frac{\kappa_1}{1+\kappa_1}\Big[1 - \exp\Big(-\frac{D_1}{D_x^0}\Big)\Big], \tag{51}$$

$$y_1^{wd}(0) = 0, \tag{52}$$

$$z_1^{wd}(0) = 0, \tag{53}$$

$$x_i^{wd}(0) = 0 \qquad (i = 2, \ldots, n), \tag{54}$$

$$y_i^{wd}(0) = 0 \qquad (i = 2, \ldots, n), \tag{55}$$

$$z_i^{wd}(0) = 0 \qquad (i = 2, \ldots, n). \tag{56}$$

In these equations, $\bar{x}$, $\bar{y}$ and $\bar{z}$ are the normal concentrations of X, Y and Z cells.

At time moment T_i of the i-th ($i = 2, \ldots, n$) irradiation (recalling that $T_i = \sum_{j=1}^{i-1}\tau_j$), the concentrations of the cells under consideration take the following values:

$$x^{ud}(T_i) = \tilde{x}_i^{ud}\exp\Big(-\frac{D_i}{D_x^0}\Big) \qquad (i = 2, \ldots, n), \tag{57}$$

$$y^{ud}(T_i) = \tilde{y}_i^{ud} \qquad (i = 2, \ldots, n), \tag{58}$$

$$z^{ud}(T_i) = \tilde{z}_i^{ud} \qquad (i = 2, \ldots, n), \tag{59}$$

$$x^{hd}(T_i) = \tilde{x}_i^{hd} + \tilde{x}_i^{ud}\frac{\rho_i}{1+\rho_i}\Big[1 - \exp\Big(-\frac{D_i}{D_x^0}\Big)\Big] + \sum_{j=1}^{i-1}\tilde{x}_{ij}^{wd}\Big[1 - \exp\Big(-\frac{D_i}{D_{xwd}^{00}}\Big)\Big] + \tilde{x}_i^{md}\Big[1 - \exp\Big(-\frac{D_i}{D_{xmd}^{00}}\Big)\Big] \qquad (i = 2, \ldots, n), \tag{60}$$

$$x^{md}(T_i) = \tilde{x}_i^{md}\Big[\exp\Big(-\frac{D_i}{D_{xmd}^{00}}\Big)\Big] + \tilde{x}_i^{ud}\frac{1}{1+\rho_i}\frac{1}{1+\kappa_i}\Big[1 - \exp\Big(-\frac{D_i}{D_x^0}\Big)\Big] \qquad (i = 2, \ldots, n), \tag{61}$$

$$x_i^{wd}(T_i) = \tilde{x}_i^{ud}\frac{1}{1+\rho_i}\frac{\kappa_i}{1+\kappa_i}\Big[1 - \exp\Big(-\frac{D_i}{D_x^0}\Big)\Big] \qquad (i = 2, \ldots, n), \tag{62}$$

$$y_i^{wd}(T_i) = 0 \qquad (i = 2, \ldots, n), \tag{63}$$

$$z_i^{wd}(T_i) = 0 \qquad (i = 2, \ldots, n), \tag{64}$$

$$x_j^{wd}(T_i) = \tilde{x}_{ij}^{wd}\exp\Big(-\frac{D_i}{D_{xwd}^{00}}\Big) \qquad (j = 1, \ldots, i-1; i = 2, \ldots, n) \tag{65}$$

$$y_j^{wd}(T_i) = \tilde{y}_{ij}^{wd} \qquad (j = 1, \ldots, i-1; i = 2, \ldots, n), \tag{66}$$

$$z_j^{wd}(T_i) = \tilde{z}_{ij}^{wd} \qquad (j = 1, \ldots, i-1; i = 2, \ldots, n), \tag{67}$$

where $\tilde{x}_i^{ud}, \tilde{y}_i^{ud}, \tilde{z}_i^{ud}, \tilde{x}_i^{hd}, \tilde{x}_i^{md}, \tilde{x}_{ij}^{wd}, \tilde{y}_{ij}^{wd}$ and $\tilde{z}_{ij}^{wd}$ ($j = 1, \ldots, i-1$; $i = 2, \ldots, n$) are the concentrations of X^{ud}, Y^{ud}, Z^{ud}, X^{hd}, X^{md}, X_j^{wd}, Y_j^{wd}, and Z_j^{wd} ($j = 1, \ldots, i-1$) cells just before the i-th irradiation performed at time moment T_i ($i = 2, \ldots, n$).

The parameter ρ_i ($i = 1, \ldots, n$) in Eqs. (49–51) and Eqs. (60–62) is the ratio of the fractions of undamaged X^{ud} cells, which transfer to heavily damaged X^{hd} cells and to moderately damaged X^{md} cells and weakly damaged X_i^{wd} ($i = 1, \ldots, n$) cells, respectively, after the i-th ($i =$

TABLE 1
Parameters of the Model of the Human Small Intestinal Epithelium

Parameter	Value	Dimension
α	5.6	Day^{-1}
γ	0.44	Day^{-1}
δ	1.4	Day^{-1}
ψ	0.5	Day^{-1}
μ	0.5	Day^{-1}
ν	6.0	Day^{-1}
η	0.1	Day^{-1}
σ	1.25	Day
λ	1.25	Day
τ_{ar}	10	Day
υ	0.001	$DayGy^{-1}$
ϕ	1	1
φ	3	1
ς	1	1
ϑ_y	0.1	1
ϑ_z	25	1
D_x^0	4	Gy
D_x^{00}	70	Gy
D_x^{000}	40	Gy

1, . . ., n) irradiation with a dose D_i ($i = 1, \ldots, n$). By virtue of Eq. (32), it reads as:

$$\rho_i = \frac{1 - \exp(-D_i/D_x^{00})}{\exp(-D_i/D_x^{00}) - \exp(-D_i/D_x^{0})} \qquad (i = 1, \ldots, n). \quad (68)$$

The parameter κ_i ($i = 1, \ldots, n$) in Eqs. (43), (44), (54) and (55) is the ratio of the fractions of undamaged X^{ud} cells, which transfer to weakly damaged X_i^{wd} ($i = 1, \ldots, n$) cells and to moderately damaged X^{md} cells after the i-th ($i = 1, \ldots, n$) irradiation with a dose D_i ($i = 1, \ldots, n$). By virtue of Eq. (33), it reads as:

$$\kappa_i = \frac{\exp(-D_i/D_x^{000}) - \exp(-D_i/D_x^{0})}{\exp(-D_i/D_x^{00}) - \exp(-D_i/D_x^{000})} \qquad (i = 1, \ldots, n). \quad (69)$$

Here the parameters D_x^0, D_x^{00} and D_x^{000} are specified above. The parameters D_{xwd}^{00} and D_{xmd}^{00} characterize the radiosensitivity of weakly damaged X_j^{wd} ($j = 1, \ldots, i-1$; $i = 2, \ldots, n$) cells and the moderately damaged X^{md} cells, respectively. Specifically, D_{xwd}^{00} is the dose, after exposure to which the number of X_j^{wd} ($j = 1, \ldots, i-1$; $i = 2, \ldots, n$) cells that did not undergo the interphase death is $e = 2.718\ldots$ times smaller than their initial number (*1*). The coefficient D_{xmd}^{00} is the dose, after exposure to which the number of moderately damaged cells (X^{md} cells) that did not undergo the interphase death is $e = 2.718\ldots$ times smaller than their initial number (*1*). For the sake of simplicity, it is natural to assume that the values of D_{xwd}^{00} and D_{xmd}^{00} are equal to D_x^{00}.

The values of the independent parameters of the developed model of the human small intestinal epithelium are given in Table 1. The parameters μ, η, ν, γ, δ, ψ and D_x^0 are determined proceeding from the literature data (*1, 18–20*). The values of the parameters α, σ, λ and ϑ_y are taken to be the same as those in the model of the mouse small intestinal epithelium, the first three of them being determined proceeding from the literature data [see (*9, 10*) and references therein for the details]. The values of the parameters τ_{ar}, υ, ϕ, φ, and ς are taken the same as those in the model of the other epithelium, namely, the skin epidermal epithelium in young swine, which bears many characteristics similar to the skin epidermal epithelium in humans (*10, 14, 15*). The values of the parameters ϑ_z, D_x^{00} and D_x^{000} are evaluated by matching the modeling results with the empirical data (*4*).

The developed model [Eqs. (5), (6), (34–69)] is rewritten, for the convenience, in terms of the new dimensionless variables, the latter being the ratios of the dimension concentrations of the small intestinal epithelial cells considered in the model to their normal values. For the numerical study of the model, a Fortran program is elaborated.

It is worthwhile to note that the developed model [Eqs. (5), (6), (34–69)], which describes the dynamics of the human small intestinal epithelium under n-fractionated irradiation, is reduced to Eqs. (5), (6), (10–33), which describe the dynamics of this vital body system under acute exposure, if n is taken to be equal to unity and the parameter D_1 is considered as the acute dose of radiation D. In turn, Eqs. (5), (6) and (10–33) are reduced to Eqs. (1–9), which describe the dynamics of this system under normal conditions, if the parameter D entering Eqs. (5), (6) and (10–33) is taken to be equal to zero. Thus, the developed model of the small intestinal epithelium can be used in the studies of the dynamics of this vital body system under normal conditions, under acute irradiation, and under n-fractionated irradiation.

RESULTS AND DISCUSSION

The model is applied to the numerical study of the dynamics of the normal non-cancerous small intestinal epithelium in patients who underwent n-fractionated exposures. Scenarios of n-fractionated exposure, which are used in this modeling study, are reconstructed proceeding from the sets of parameters of fractionated irradiation of patients, which are reported elsewhere(*4*). Specifically, a set of such parameters given elsewhere (*4*) for a patient includes the total radiation therapy duration of 28 days, the fraction number of 24 (six fractions per week), and the doses of 0.96, 2.88, 6.24, 17.28, 24.96, 31.68 Gy accumulated over days 1, 4, 8, 15, 22, 28 from the onset of exposure, respectively. These data allow one to reconstruct a plausible set of fraction doses for this patient (Table 2). In turn, sets of parameters of fractionated exposures of other patients, which are reported elsewhere (*4*), include the total radiation therapy duration, the fraction number, the number of fractions per week, and total radiation dose. These data allow one to reconstruct the scenarios of fractionated exposures for those patients. For the sake of simplicity, it is supposed that the fraction dose is the same during the entire period of radiation therapy for each of those patients and it is equal to the ratio of the respective total dose to the respective fraction number.

The empirical data are given elsewhere (*4*) as the sets of epithelial counts (epithelial surface area). One set includes a pretreatment value and several values for the time moments during and after radiation therapy. The other ones include only a pretreatment value, minimal value and value measured two weeks after the end of radiation therapy. Keeping in mind that, 1. the small intestinal epithelium represents a single-cell-layer epithelium and 2. villous cells and crypt cells (via openings called crypt ostia) have access to the epithelial surface, the measured epithelial counts characterize the epithelial cell counts. Proceeding from this, the empirical data (*4*), which are given in Figs. 1–4 in the dimensionless form as the ratio of the reported epithelial counts to the respective pretreatment epithelial count, are compared with the relevant modeling results on the dynamics of the dimensionless total concentration of X, Y and Z cells, which are also displayed in these figures.

TABLE 2
Reconstructed Scenario of a Patient Receiving Fractionated Irradiation (*4*)

Day of radiation therapy	Fraction dose (Gy)
1	0.96
2	0.96
3	0.48
4	0.48
5	-
6	0.96
7	0.96
8	1.44
9	1.44
10	1.92
11	1.92
12	-
13	1.92
14	1.92
15	1.92
16	1.92
17	1.92
18	0.96
19	-
20	0.96
21	0.96
22	0.96
23	1.44
24	1.44
25	1.44
26	-
27	1.44
28	0.96

As one can conclude from Figs. 1–4, the modeling results are in agreement with the respective empirical data. Namely, the dimensionless concentration of the epithelial cells decreases, reaches the minimal level and then returns to the normal level. It is important to note that the time required for recovering the normal level of the epithelial cells, which is obtained in the model for all considered scenarios of exposure, is approximately two weeks post-radiation therapy, which also conforms to the empirical data.

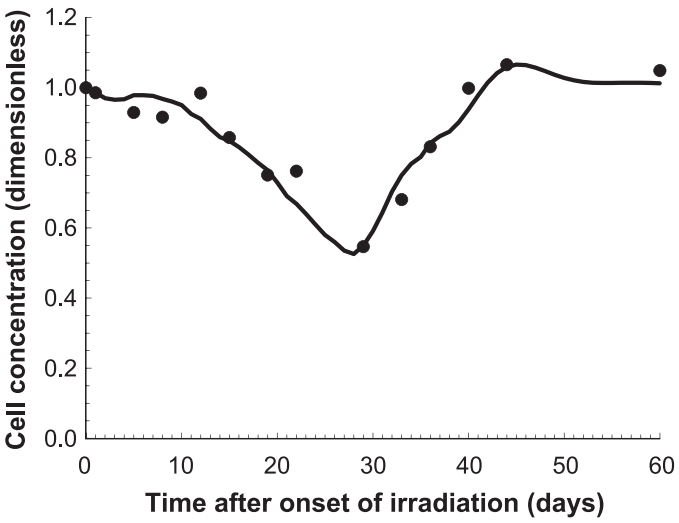

FIG. 1. The modeling results (curve) on the dynamics of the dimensionless concentration of the small intestinal epithelial cells in a patient treated with radiation therapy. The results were obtained for the fractionated irradiation scenario specified in Table 2. Solid circles indicate the corresponding empirical data for that patient, reported elsewhere (*4*).

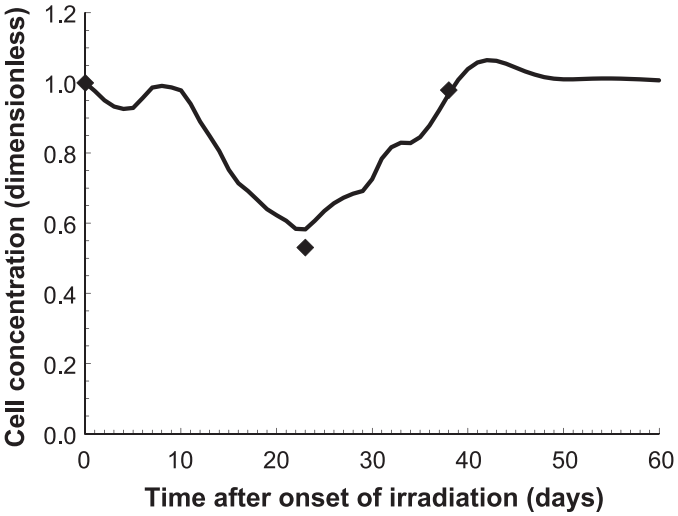

FIG. 2. The modeling results (curve) on the dynamics of the dimensionless concentration of the small intestinal epithelial cells in a patient treated with radiation therapy. The results were obtained for the fractionated irradiation scenario with total duration of 24 days, 18 fractions (five fractions per week), total dose of 28.8 Gy and fraction dose of 1.6 Gy. Solid diamonds indicate the corresponding empirical data for that patient (*4*).

The agreement of the modeling results with the corresponding empirical data obtained for patients treated with radiation therapy (*4*) testifies to the capability of the developed model of predicting the dynamics of the small

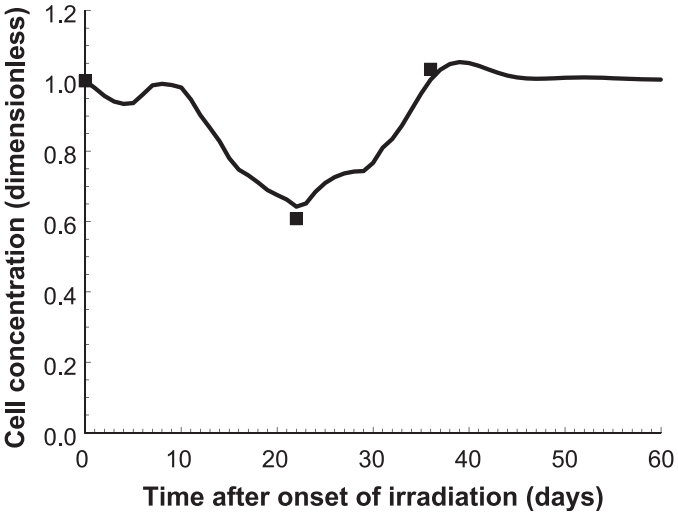

FIG. 3. The modeling results (curve) on the dynamics of the dimensionless concentration of the small intestinal epithelial cells in a patient treated with radiation therapy. The results were obtained for fractionated irradiation scenario with total duration of 22 days, 16 fractions (five fractions per week), total dose of 22.08 Gy and fraction dose of 1.38 Gy. Filled squares indicate the corresponding empirical data for that patient (*4*).

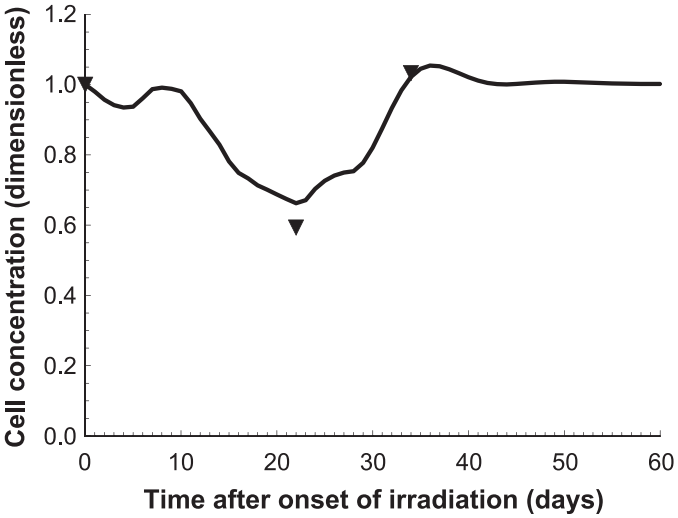

FIG. 4. The modeling results (curve) on the dynamics of the dimensionless concentration of the small intestinal epithelial cells in a patient treated with radiation therapy. The results were obtained for the fractionated irradiation scenario with total duration of 20 days, 14 fractions (five fractions per week), total dose of 19.18 Gy and fraction dose of 1.37 Gy. Solid triangles indicate the corresponding empirical data for that patient (*4*).

intestinal epithelium in humans who undergo fractionated irradiation.

Hypofractionated Irradiation Predictions

For illustrative purposes, the model is employed in the study of the dynamical response of the human normal small intestinal epithelium to hypofractionated irradiation. The latter is characterized by a higher fraction dose and smaller number of fractions with respect to those used in the conventional fractionated irradiation. Hypofractionated irradiation applies, in particular, to stereotactic body radiation therapy, the use of which has increased over the years (*21*, *22*). The obtained modeling results are presented in Figs. 5–7.

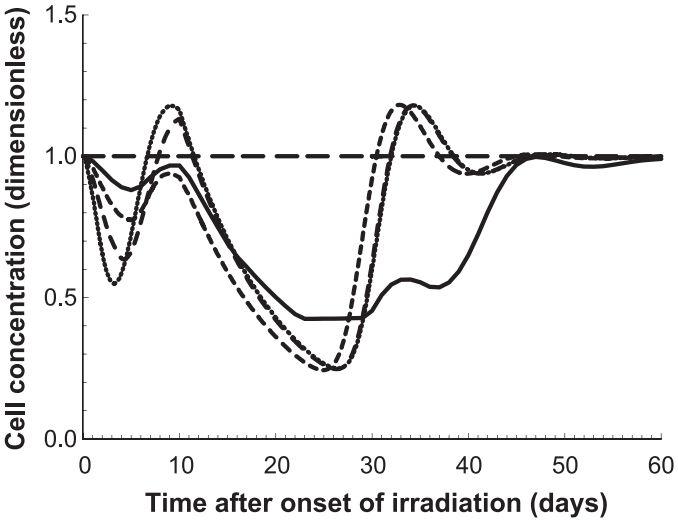

FIG. 5. The modeling results on the dynamics of the dimensionless concentration $\tilde{z}$ of the villous cells in the human normal small intestinal epithelium. Results were obtained for the conventional fractionated irradiation scenario with five fractions per week, total dose of 40 Gy and fraction dose of 2 Gy (solid curve), as well as for three scenarios of hypofractionated irradiation with five fractions per week, total dose of 40 Gy and fraction dose of 5 Gy (short-dashed curve), 10 Gy (medium-dashed curve) and 20 Gy (dotted curve). The normal level of the dimensionless concentration $\tilde{z}$ of the villous cells is indicated by the long-dashed line.

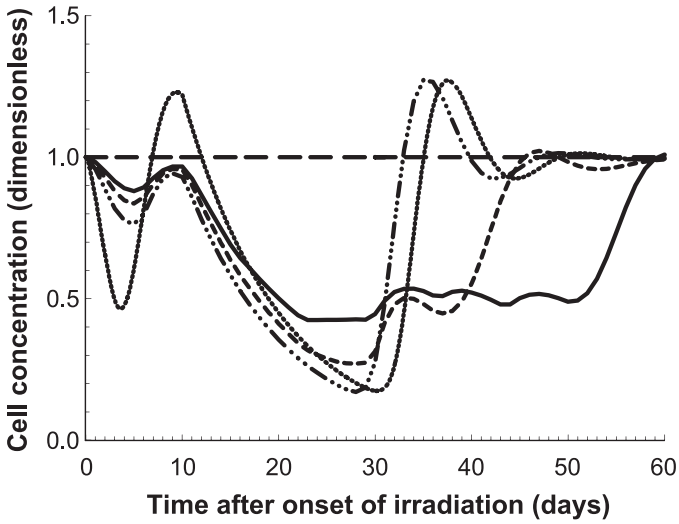

FIG. 6. The modeling results on the dynamics of the dimensionless concentration $\tilde{z}$ of the villous cells in human normal small intestinal epithelium. Results were obtained for the conventional fractionated irradiation scenario with five fractions per week, total dose of 60 Gy and fraction dose of 2 Gy (solid-line curve), as well as for three scenarios of hypofractionated irradiation with five fractions per week, total dose of 60 Gy and fraction dose of 3 Gy (short-dashed curve), 5 Gy (dot-dot-dashed curve) and 20 Gy (dotted curve). The normal level of the dimensionless concentration $\tilde{z}$ of the villous cells is indicated by the long-dashed line.

Specifically, Fig. 5 shows the modeling results on the dynamics of the dimensionless concentration $\tilde{z}$ of functional villous cells (Z cells) in the human normal small intestinal epithelium. They are obtained for one scenario of conventional fractionated irradiation and three scenarios of hypofractionated irradiation with the same total dose, same number of fractions per week and different values of the fraction dose. Note that the chosen parameters of hypofractionated irradiation correspond to those used in stereotactic body radiation therapy (*21*). As one can infer from this figure, hypofractionated irradiation with the considered parameters yields a more pronounced decrease and faster recovery of the dimensionless concentration $\tilde{z}$ of villous cells than conventional fractionated irradiation with the same total dose does.

Figure 6 shows the modeling results on the dynamics of the dimensionless concentration $\tilde{z}$ of villous cells, which are obtained for one scenario of conventional fractionated irradiation and three scenarios of hypofractionated irradiation with the same total dose (which is higher than that in Fig. 5), the same number of fractions per week and different values of the fraction dose. Note that the chosen parameters

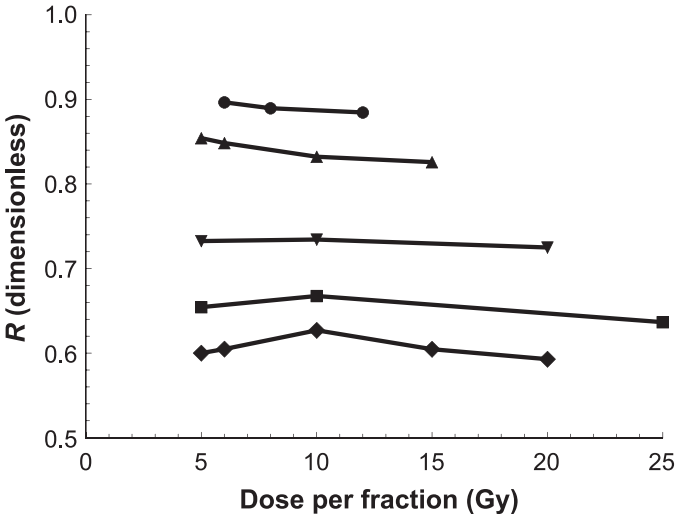

FIG. 7. The relative cumulative radiation damage effect of hypofractionated irradiation on the human normal small intestinal epithelium as a function of the fraction dose of such exposure. Modeling results were obtained for 18 scenarios of hypofractionated irradiation with the total dose of 24 Gy (circles), 30 Gy (triangles up), 40 Gy (triangles down), 50 Gy (boxes) and 60 Gy (diamonds), with fraction dose ranging from 5 to 25 Gy. In the respective scenarios of conventional fractionated irradiation, total doses are 24, 30, 40, 50 and 60 Gy, respectively, and fraction dose is 2 Gy, with five fractions per week in all the scenarios.

of two scenarios of hypofractionated irradiation correspond to those used in the stereotactic body radiation therapy (*21*), whereas the chosen parameters of the other one corresponds to those reported elsewhere (*22*). As one can conclude from Fig. 6, hypofractionated irradiation with the considered parameters also leads to a more pronounced decrease and faster recovery of the dimensionless concentration $\tilde{z}$ of villous cells than conventional fractionated irradiation with the same total dose does. The juxtaposition of the results shown in Figs. 5 and 6 implies that for the same value of the fraction dose of hypofractionated irradiation, the minimal level of $\tilde{z}$ obtained for a higher total dose (Fig. 6) is smaller than that obtained for the smaller total dose (Fig. 5) in the considered ranges of the fraction doses and the total doses.

It is important to note that for the scenario of hypofractionated irradiation with the parameters reported elswhere (*22*), the time moment, when the dimensionless concentration $\tilde{z}$ reaches its minimal level, coincides with the time moment, when the majority of patients demonstrate grades 1 and 2 of the so-called bowel toxicity (*22*). The latter characterizes the level of the bowel functional damage and thus depends on the level of the radiation-induced damage of the respective functional cells. Therefore, it is reasonable to assume that the deviation of the dimensionless concentration $\tilde{z}$ of villous cells from its normal level, being the characteristic $G(t)$ of the damage effect of such exposure on the normal small intestinal epithelium in a patient treated with radiation therapy, can, to some extent, be related to the small bowel toxicity in this patient. The function $G(t)$ reads as:

$$G(t) = 1 - \tilde{z}(t), \tag{70}$$

where the function $\tilde{z}(t)$ is computed by making use of the developed model.

Obviously, the integral of the function $G(t)$ over the period from onset of fractionated irradiation ($t = 0$) until the time of the restoration of the small intestinal epithelium ($t = t_r$), being the characteristic P of the cumulative damage effect of such exposure on the normal small intestinal epithelium in a patient treated with radiation therapy, can, to some extent, be related to the cumulative small bowel toxicity in this patient. The quantity P is determined using the following equation:

$$P = \int_0^{t_r} G(t)dt = \int_0^{t_r} (1 - \tilde{z}(t))dt. \tag{71}$$

The developed model together with Eq. (71) are used to examine the differences between the cumulative damage effects of hypofractionated radiation treatment and conventional fractionated radiotherapy with the same total dose on the human normal small intestinal epithelium. For this purpose, it is convenient to define the relative cumulative damage effect of hypofractionated radiotherapy on the human normal small intestinal epithelium, which is taken to be equal to the ratio R of the value P_H of P obtained for a scenario of hypofractionated irradiation to the value P_C of P obtained for the respective scenario of conventional fractionated irradiation:

$$R = P_H/P_C. \tag{72}$$

Here the values P_H and P_C are computed by making use of the developed model and Eq. (71). The parameters of hypofractionated irradiation used in these computations correspond to those used in the stereotactic body radiation therapy (*21*). The obtained modeling results are presented in Fig. 7.

As one can conclude from Fig. 7, the values of R are somewhat smaller than unity for all the considered regimens of hypofractionated irradiation. In turn, the values of R are smaller for higher values of the total dose for the considered ranges of total doses and fraction doses. These modeling findings demonstrate that the hypofractionated irradiation yields a somewhat less pronounced cumulative damage effect on the human normal small intestinal epithelium (which can be related to the cumulative small bowel toxicity) than conventional fractionated irradiation with the same total dose.

CONCLUSIONS

In this work, a biologically motivated mathematical model of the dynamics of the small intestinal epithelium in humans treated with fractionated radiotherapy was developed. It is implemented as a system of nonlinear ordinary differential equations, in which variables and parameters have a clear biological meaning. The principal

advantage of the developed model is the explicit incorporation of the key kinetic and radiobiological parameters of the human small intestinal system, as well as the key parameters of fractionated irradiation (fraction dose, fraction number and time intervals between fractions).

The performed studies revealed that the patterns of the modeling dynamics of the small intestinal epithelium, obtained for fractionated radiotherapy scenarios in which patients receive total dose spanning the range of 19.20 ÷ 31.68 Gy, fraction number spanning the range of 14 ÷ 24 and total therapy duration spanning the range of 20 ÷ 28 days (*4*), agree with the respective empirical data obtained for the normal non-cancerous small intestinal tissue of those patients (*4*). The obtained agreement testifies to the capability of the developed model for predicting the dynamical response of the human small intestinal epithelium to fractionated irradiation. It is also revealed that in the considered ranges of total doses and fraction doses the cumulative damage effect of hypofractionated irradiation on the human normal small intestinal epithelium, which can be related to the cumulative small bowel toxicity, is somewhat less pronounced than that of conventional fractionated irradiation with the same total dose.

All this bears witness to the validity of employing the developed model in the investigation and prediction of radiation-induced side effects on the normal non-cancerous small intestinal tissue in patients with intra-abdominal and pelvic malignancies, who undergo fractionated radiation therapy. Such predictions could help in choosing appropriate fractionated radiation therapy regimens for minimizing side effects on the normal small bowel. The developed model is also capable of describing the effects of acute radiation on the human small intestinal epithelium, which could help to predict potential health hazards for an individual irradiated in the result of accidents or incidents, and thus, to select an appropriate treatment. Another application for the developed model is the prediction of damage to the small intestinal epithelium in astronauts caused by radiation incidents, which may occur during long-term interplanetary space missions (e.g., voyages to Mars or Lunar colonies). The obtained modeling predictions would provide a better understanding of the health risks of astronauts and enable one to evaluate the need for operational applications of countermeasures.

Received: April 29, 2019; accepted: July 10, 2019; published online: August 15, 2019

REFERENCES

1. Bond VP, Fliendner TM, Archambeau JO. Mammalian radiation lethality: a disturbance in cellular kinetics. New York: Academic Press; 1965.
2. Becciolini A. Relative radiosensitivities of the small and large intestine. In: Lett JT, Altman KL, editors. Advances in radiation biology. Relative radiation sensitivities of human organ systems. Vol. 12. Orlando: Academic Press Inc.; 1987. p. 83–128.
3. Carr KE. Effects of radiation damage on intestinal morphology. Int Rev Cytol 2001; 208:1–119.
4. Trier JS, Browning TH. Morphologic response of the mucosa of human small intestine to X-ray exposure. J Clin Invest 1966; 45:194–204.
5. Shadad AK, Sullivan FJ, Martin JD, Egan LJ. Gastrointestinal radiation injury: Symptoms, risk factors and mechanisms. World J Gastroenterol 2013; 19:185–98.
6. Shadad AK, Sullivan FJ, Martin JD, Egan LJ. Gastrointestinal radiation injury: Prevention and treatment. World J Gastroenterol 2013; 19:199–208.
7. Yu J. Intestinal stem cell injury and protection during cancer therapy. Transl Cancer Res 2013; 2:384–96.
8. Kim CK, Vincent W, Yang VW, Bialkowska AB. The role of intestinal stem cells in epithelial regeneration following radiation-induced gut injury. Curr Stem Cell Rep 2017; 3:320–32.
9. Smirnova OA. Blood and small intestine cell kinetics under radiation exposures: mathematical modeling. Adv Space Res 2009; 44:1457–69.
10. Smirnova OA. Environmental radiation effects on mammals: a dynamical modeling approach. New York: Springer; 2017.
11. Delgado ME, Grabinger T, Brunner T. Cell death at the intestinal epithelial front line. FEBS J 2016; 283: 2701–19.
12. Parker A, Maclaren OJ, Fletcher AG, Muraro D, Kreuzaler PA, Byrne HM, et al. Cell proliferation within small intestinal crypts is the principal driving force for cell migration on villi. FASEB J 2017; 31:636–49.
13. Kong S, Zhang YH, Zhang W. Regulation of intestinal epithelial cells properties and functions by amino acids. Biomed Res Int 2018; 2018:2819154.
14. Smirnova OA, Hu S, Cucinotta FA. Dynamics of acutely irradiated skin epidermal epithelium in swine: modeling studies. Health Phys 2014; 107:47–59.
15. Smirnova OA, Cucinotta FA. Skin response to single and fractionated irradiation: dynamic modeling approach. Health Phys 2016; 111:513–27.
16. Lea DE. Action of radiation on living cells. Cambridge: The Syndics of the Cambridge University Press; 1955.
17. Oldham KB, Myland JC, Spanier J. An atlas of functions. New York: Springer; 2009.
18. Wright N, Watson A, Morley A, Appleton D, Marks J, and Douglas A. The cell cycle time in the flat (avillous) mucosa of the human small intestine. Gut 1973; 14:603–6.
19. Van der Wath RC, Gardiner BS, Burgess AW, Smith DW. Cell organization in the colonic crypt: A theoretical comparison of the pedigree and niche concepts. PLoS One 2013; 8:e73204.
20. Aleksandrov Yu A. The basics of radiation ecology. Yoshkar-Ola: MarSU; 2007.
21. Thomas TO, Hasan S, Small Jr W, Herman JM, Lock M, Kim EY, et al. The tolerance of gastrointestinal organs to stereotactic body radiation therapy: what do we know so far? J Gastrointest Oncol 2014; 5:236–46.
22. Wilson JM, Dearnaley D, Syndikus I, Khoo V, Birtle A, Bloomfield D, et al. The efficacy and safety of conventional and hypofractionated high-dose radiation therapy for prostate cancer in an elderly population: a subgroup analysis of the CHHiP trial. Int J Radiat Oncol Biol Phys 2018; 100:1179–89.